Extended Abstracts of the 2018 International Conference on Solid State Devices and Materials, Tokyo, 2018, pp1047-1048

Highly Efficient Planar Perovskite Solar Cells Utilizing Electron Transport Bilayer

Md. Shahiduzzaman,[1,2*] Hiroto Ashikawa,[1] Mizuki Kuniyoshi,[1] Sem Visal,[1] Tetsuya Kaneko,[1] Tetsuhiro Katsumata,[1] Tetsuya Taima,[2] Satoru Iwamori,[1] Masao Isomura,[1*] and Koji Tomita[1*]

[1]Tokai Univ.,
Hiratsuka, Kanagawa 259-1292, Japan
[2]Kanazawa Univ.,
Kakuma, Kanazawa 920-1192, Japan

Phone : +81-463-58-1211(ext.3742) E-mail : shahiduzzaman@tokai.ac.jp; isomura@tokai-u.jp; tomita@keyaki.cc.u-tokai.ac.jp

Abstract

Herein, we report a facile method for enhancing the performance of planar heterojunction perovskite solar cells by inserting a compact TiO_2/Anatase (AT) TiO_2 NPs bilayer, respectively, by spray pyrolysis (SP) deposition and spin-coating (SC) technique. The improved photovoltaic performance of devices with an SP-TiO_2/SC-AT TiO_2 NPs bilayer facilitated more efficient electron transport, charge extraction, and low interfacial recombination, and ultimately yields champion efficiencies up to 17.05% by a significant decrease of *J-V* hysteresis, presenting almost 12% enhancement compared to the TiO_2 single layer-based counterparts.

1. Introduction

Kojima *et al*. first introduced perovskite solar cells (PSCs) in 2009 with a power conversion efficiency (PCE) of 3.8% [1]. This encouraging discovery led to further performance enhancements, resulting in a remarkable efficiency of 22.7% at the present date [2].

In this study, we report a novel, higher potential and environmental friendly approach for preparing single-crystalline anatase (AT) TiO_2 NPs by a simple, scalable one-step hydrothermal route [3] using water-soluble titanium complex as a titanium source. The resultant AT TiO_2 NPs performs as electron transport layer (ETL) bilayer in planar heterojunction (PHJ) PSCs.

2. Materials and Method

Titanium fine powder of 10 mmol was dissolved in the mixed solution of 30%-H_2O_2 aq. and 28%-NH_3 aq., then malic acid of 10 mmol was added here. After the solution was dried at 50 °C in order to remove excess H_2O_2 and NH_3, 0.5 M Ti-malate complex solution was prepared by adding distilled water. The Ti complex solution was heat-treated in an autoclave at 200 °C for 5 h. Formed TiO_2 particles were separated by centrifuge and washed with distilled water twice. TiO_2 NPs were dispersed in distilled in water. Then, AT TiO_2 NPs layer was placed on the compact spray-pyrolysis (SP) deposited TiO_2 layer by spin-coating (SC) method and annealed at 100 °C for 5 min, followed by sintered at 450 °C for 30 min in a muffle furnace. Finally, a compact SP-TiO_2/SC- AT TiO_2 NPs bilayer was obtained by combining SP deposition and SC technique, respectively, and used as ETLs. The perovskite precursor solution (1M PbI_2 and 1M CH_3NH_3I in DMF and DMSO mixed solvent) was coated on the resulting substrates. The precursor coated substrates were then allowed to anneal at 100 °C on a hot plate for 1 h to crystallize perovskite. The optimized thickness of SP-TiO_2, SC-AT TiO_2 (three cycle-coating), perovskite layer, Spiro-OMeTAD and Au layers were measured ~70, ~50, ~270, ~250, and ~60 nm, respectively.

3. Results and Discussion

The as-synthesized nocrystalline AT TiO_2 NPs can formulate stable (more than a month) nonocolloidal solutions in aqueous media (inset of **Fig. 1a**; concentration = 10 mg/mL). The XRD pattern of AT-TiO_2 is depicted in **Fig. 1a**. Thus, confirms as-synthesized TiO_2 NPs indeed comprise a significant amount of the AT domains. The resultant AT TiO_2 NPs film exhibits well-behaved optical transparency, with transmittance greater than 80% over the entire visible region (**Fig. 1b**). To gain further insights into nanoscale morphology and sizes of AT TiO_2 NPs, scanning transmission electron microscopy (STEM) has been performed as shown in inset **Figure 1b.** The STEM image reveals that the AT TiO_2 NPs is spherical-like, with a particle size ranging from 6 to 10 nm in diameter. The XRD patterns of the perovskite films formed with, and without bilayer are depicted in **Figure 2.** The single SP-TiO_2 layer based-perovskite film yields a poly-crystalline morphology with a grain size of average around 351 nm, whereas the SP-TiO_2/SC-AT TiO_2 NPs bilayer based-perovskite film reveals an average grain size of 765 nm, respectively, as estimated full-width half maximum (FWHM) from whole pattern fitting method using the Scherrer equation and resultant values are consistent with the top-view morphologies as shown in the SEM images in **Fig. 3c and 3d.** Interfacial modification of compact SP-TiO_2 by a novel single-crystalline SC-AT TiO_2 NPs layer with the 50-nm-thickness is homogenously distributed, followed by uniform and denser scaffolds of SP-TiO_2/SC-AT TiO_2 NPs bilayer (**Figure 3b**) without visible cracks and thus offers more efficient the separation of charges and suppresses the

recombination rate.

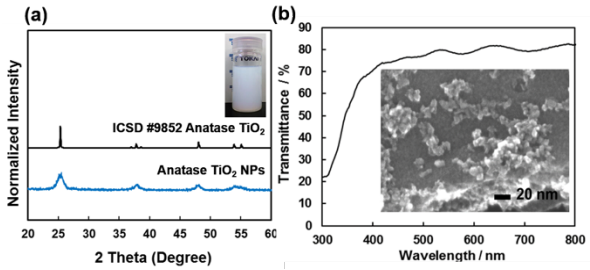

Fig. 1. (a) XRD pattern of AT TiO_2 NPs. Inset shows AT TiO_2 nonocolloidal solutions vial in aqueous media; (b) Transmittance spectra of SC-AT TiO_2 NPs film. Inset showing a representative STEM image of SC-AT TiO_2 NPs deposited on FTO/glass substrate.

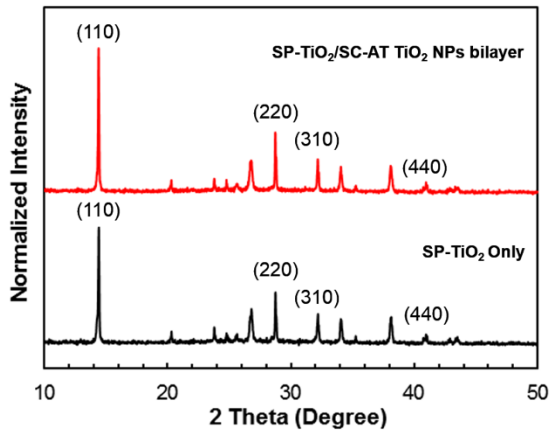

Fig. 2. The XRD patterns of perovskite films formed with single SP-TiO_2 layer and SP-TiO_2/SC-AT TiO_2 NPs bilayer.

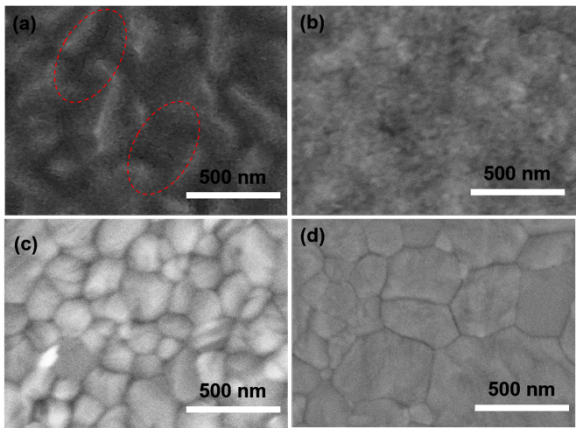

Fig. 3. Top view of SEM images of (a) SP-TiO_2 and (b) SP-TiO_2/SC-AT TiO_2 NPs bilayer; perovskite films grown on (c) SP-TiO_2 and (d) SP-TiO_2/SC-AT TiO_2 NPs bilayer layer.

The photoluminance (PL) measurement reveals that the PL of perovskite is quenched significantly in the presence of SP-TiO_2/SC-AT TiO_2 NPs bilayer as shown in **Fig. 4.** The PL for SP-TiO_2/SC- AT TiO_2 NPs/perovskite film shows a stronger quenching, revealing efficient charge transfer at the interface between the photo-excited perovskite and SP-TiO_2/SC-AT TiO_2 NPs bilayer.

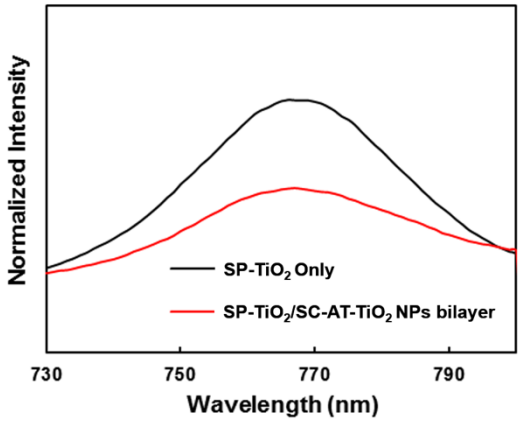

Fig. 4. PL spectra of perovskite films deposited on with or without bilayers.

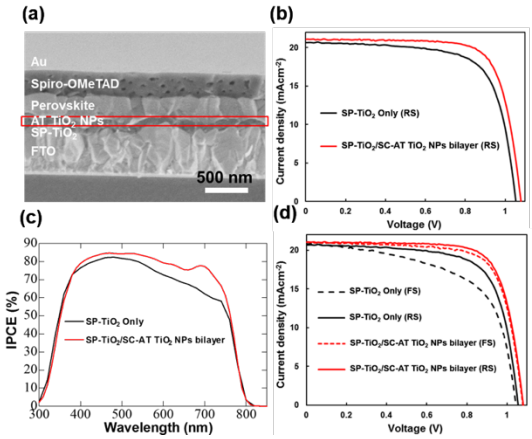

Fig. 5. (a) A cross-sectional SEM image of the PSCs processed with TiO_2 NPs-based bilayer. (b) Reverse-scan (RS) *J-V* curves obtained for solar cells based on with and without bilayer. (c) IPCE spectra of representative devices. (d) Forward-scan and RS *J-V* characteristics of solar cells.

The SP-TiO_2 singled layer-based champion (RS) PSCs exhibited considerably low a J_{sc} of 20.68 $mAcm^{-2}$, V_{oc} of 1.05 V, FF of 0.70, and PCE of 15.33% as shown in **Fig. 5b**. In contrast, the FF was enhanced from 0.70 to 0.75 upon the inclusion of SP-TiO_2/SC-AT TiO_2 NPs bilayer. We assumed that the performance enhancement of a device utilizing bilayer ETL is caused by the high content of the nanocrystalline AT phase within the compact layer and the highly homogeneous morphology that favored together with electron extraction by reducing the rate of carrier recombination, compared to that of SP-TiO_2 single layer.

Conclusions

The optimized three cycle-coating layers of SC-AT TiO_2 NPs on SP-TiO_2 based devices yield the maximum PCE of 17.05% was obtained for the resulting PSCs.

Acknowledgements

This study was supported in part by Research and Study Project of Tokai University General Research Organization.

References

[1] A. Kojima, K. Teshima, Y. Shirai and T. Miyasaka, J. Am. Chem. Soc. **131** (2009) 6050.

[2] https://www.nrel.gov/pv/assets/images/efficiency-chart.png vol. (accessed 2018).

[3] K. Tomita, V. Petrykin, M. Kobayashi, M. Shiro, M. Yoshimura, M. Kakihana, Angew. Chem. Int. Ed **45** (2006) 2378.